

Synthetic and Characterization of Al-PTFE Functionally Graded Material Using Powder Metallurgy Technique

Ghufran Hamza Omran

University of Babylon
College of Engineering
Mechanical Eng. Dept., Babylon
Iraq

Nabaa Sattar Radhi

University of Babylon
College of Engineering
Mechanical Eng. Dept., Babylon
Iraq

Basim Ajeel Abass

University of Babylon
College of Engineering
Mechanical Eng. Dept., Babylon
Iraq

The current work involves producing the functionally graded material (Al-PTFE) utilizing the powder metallurgy technique. The proposed graded materials include three, four, and five layers. Each layer consists of PTFE and Al particles with an average diameter of 200nm and 25 micrometers, respectively. The powders were blended, formed into cylindrical shapes, and then sintered in an inert environment furnace. The microstructural and morphological properties of the graded materials are studied using XRD and SEM images. The prepared graded materials' porosity density and hardness are measured experimentally. The results of XRD and SEM images reveal that the FGMs are successfully developed without any separation or crack formation and that PTFE was uniformly dispersed throughout the layers with particle concentrations of 25 and 50 wt%. Al. The obtained results also reveal that the density of various FGMs was comparable to that of PTFE.

Keywords: Composite material, FGM, Powder compaction, physical properties, PTFE, Al.

1. INTRODUCTION

Advanced engineering applications need a new material rather than a single composition, which cannot satisfy the required specifications [1]. FGMs are advanced composite materials with progressive changes in design and structure through size and tailored properties with great demands in engineering applications [2]. Preparation of FGM for adjusting the physical and mechanical properties is a challenging task for the workers in this field. Different methods are used for developing FGMs, such as coating, centrifugal casting, and powder metallurgy. Among these methods, Powder metallurgy (PM) is more efficient for producing gradients without flaws [3-6]. The critical process to get the required specifications of the FGM is the sintering of green compact. It represents a challenge due to the different thermal expansion of the materials. Many works have been implemented to study the effect of sintering on the characteristics of the FGMs [7-9]. The excellent design of FGMs leads to a smooth transition of properties [10, 11]. Metal polymer was used as a bearing material to substitute the conventional bi-metal bearings in several lubrication applications due to its hardness and wear resistance [12]. Yang et al. [13] constructed an organic/inorganic PTFE/Al³⁺-MXene bi-layer coating with excellent lubricating properties and long service life fabricated by a two-step strategy. The influences of pre-friction time on the morphology and flatness of

PTFE/Al³⁺-MXene/T-1 heterogeneous coating were investigated. Wu et al. [14] examined Al-PTFE composites' mechanical properties and reactivity with different Al Particle sizes. The stress-strain data under quasistatic compression demonstrates that as the Alparticle's size increased, the Al-PTFE specimen's strength declined. It was observed that the toughness of the material roses initially and subsequently decreased. Sahli et al. [15] prepared and characterized (PTFE)/Thermally Expanded Graphite composite (TEG). The findings showed that utilizing a higher concentration of TEG raised the glass-transition temperature of the composite. The mechanical properties improvement of functionally graded bearing materials produced by horizontal centrifugal casting was extensively studied [16,17]. The fabricated composites can replace conventional leaded bearing materials with superior copper functionally graded composites with better wear and mechanical characteristics. Srinivas et al. [18] studied the microstructural, mechanical, and tribological features of the Al-based functionally graded material fabricated by powder metallurgy. It was discovered that the mechanical characteristics of FGM highly depend upon the sintering temperature and slightly on compacting pressure and sintering time. Polytetrafluoroethylene is commonly used as a bearing material due to its superior coefficient of friction, corrosion resistance, ability to work under a wide range of temperatures, and high self-lubricating characteristics. Its high wear rate severely restricts its uses in this field [19]. This material's high toughness and flexibility make it appropriate for sealing parts [20]. It was found that employing different types of fillers, such as copper [21], Al-SiC [22], carbon [23], and MoS₂ [24], can alter the tribological properties of PTFE. Zidaru et al.[25], studied the improvements of tribolo-

Received: September 2023, Accepted: November 2023

Correspondence to: Prof. Dr Basim A. Abass
University of Babylon, College of Engineering,
Mechanical Eng. Dept., Babylon, Iraq.
E-mail:eng.basim.ajeel@uobabylon.edu.iq

doi: 10.5937/fme24010570

© Faculty of Mechanical Engineering, Belgrade. All rights reserved

FME Transactions (2024) 52, 57-67 57

gical behavior in three cone bits bearings. Amsler machine A135 was used to establish the bearing material friction coefficient and wear when lubricated with the PTFE greases. Keshavamurthy et al. [26] investigated the behavior of copper-polymer composite material developed by fused deposition modeling. Worn-out surfaces were subjected to scanning electron microscopy studies to analyze and identify the possible wear mechanisms. Soni et al. [27] explored the microstructure, machinability, and mechanical properties of the Al7075 alloy reinforced by 1wt% microsized SiC particles and 0.5wt% of h-BN nanoparticles. The outcomes of the machinability analysis for hybrid nanocomposites are compared with those of Al7075. Fragassa et al. [28] produced defect-free high-density polyurethane (PU) for use in an innovative solar vehicle. Successful materials have been synthesized. Poly-tetra-fluoro-ethylene (PTFE) was used in biomedical applications due to its biocompatibility, corrosion resistance, chemical inertness, and comparatively low cost [29]. It can also be used in bearing applications. However, PTFE has a higher wear rate under the applied load and rubbing speeds. So, adding aluminum particles can improve the wear rate of this material. However, pure Aluminum suffers from the highest friction coefficient compared to its alloy [30], which can be enhanced due to the existence of a low friction coefficient material such as PTFE. The present study focuses on producing functionally graded metal polymer (Al-PTFE) material using powder metallurgy technique with an inert environment sintering, which was not implemented in the previous works mentioned above. Functionally graded materials are novel materials with unique characteristics where the properties change gradually with position. Three, four, and five multi-layer functionally graded composite samples with various Al and PTFE contents were experimentally produced and tested. The powder compaction was implemented using a mold consisting of a punch, filling chamber, and bottom base designed for this purpose. Such materials' microstructure, density, porosity, and hardness have been experimentally measured.

2. EXPERIMENTAL PROCEDURE

The required materials and the experimental procedure needed to produce the functionally graded materials with different layers are presented in the following sections.

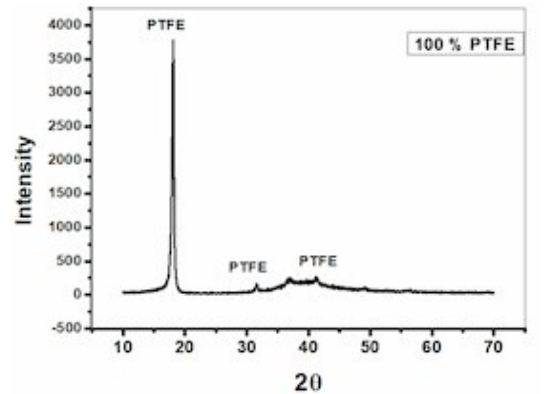
2.1 Powder characterization

Different weight percentages of 99% pure aluminum and 99% pure PTFE powders with average diameters of 25 μm and 200 nm were used to produce the required functionally graded materials. Table (1) lists the physical characteristics of such powders.

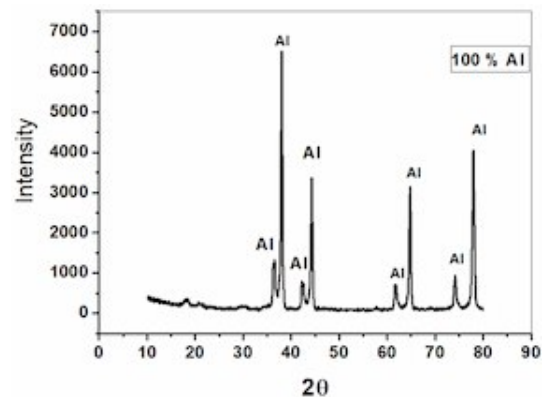
Table 1. Physical properties of Al and PTFE powders

Powder	Al	PTFE
Density g/cm^3	2.7	2.2
Melting temperature $^{\circ}\text{C}$	660.3	327
Particle size	25 μm	200 nm
Purity%	99.9	99.9

The PTFE and AL powder types were confirmed by performing the XRD test for each powder, as shown in Figure 1. Figure 1(a) illustrates the diffraction peaks 18°, 31.5°, 37°, 41°, 49°, and 70° match the PTFE standard card for Polytetrafluoroethylene (00-047-2217). Also, the diffraction peaks 19°, 39°, 41°, 65°, and 79° illustrated in Figure 1(b) match the Al standard card (00-004-0787). The XRD was implemented using the diffractometer shown in Figure 1(c).



(a)



(b)

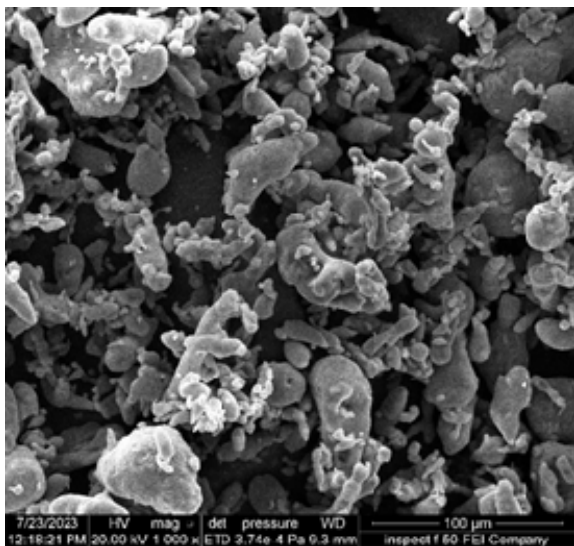
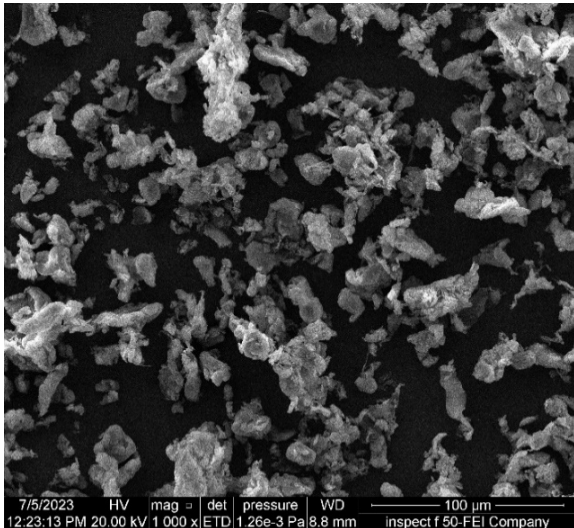


(c)

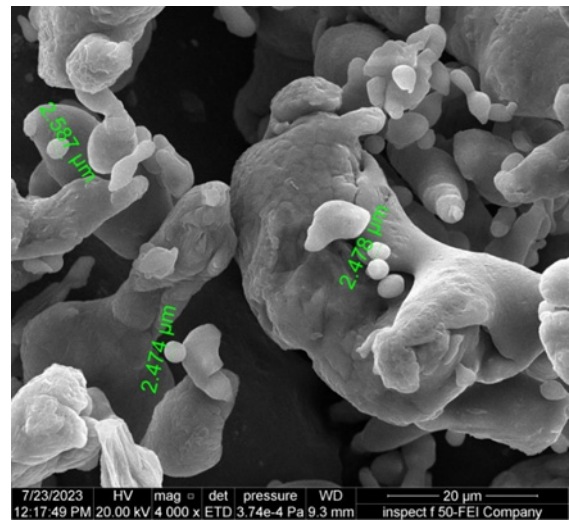
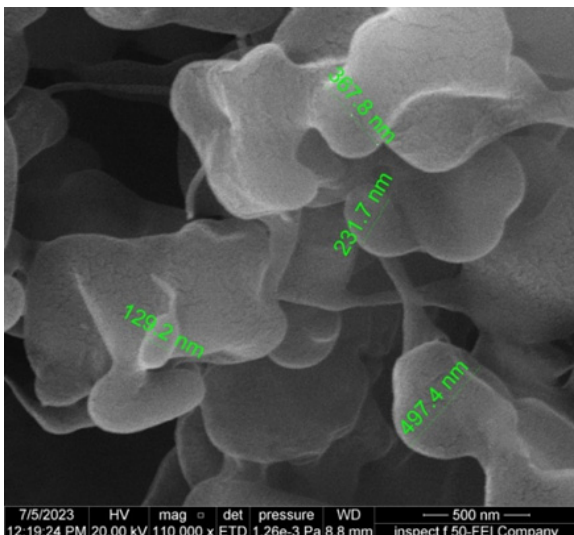
Figure 1. XRD for the powders used (a) PTFE powder (b) Al powder (c) XR Diffractometer

The morphological properties of the powders affecting their technological properties are studied using a scanning electron microscope (SEM). Figures 2(a) and Figure 2 (b) show the SEM images of the PTFE and

aluminum powders used in the present work. It can be observed from Figure 2 (a) that the PTFE particles have irregular shapes with variable grain sizes. In contrast, Figure 2(b) shows that the aluminium particles have semi-spherical shapes of different sizes. These images have been taken using the FESEM type INSPECTF50 shown in Figure 2(c).



(a)



(b)



Figure 2. SEM image of materials used (a) PTFE powder (b) Aluminium powder (c) FESEM INSPECT F50

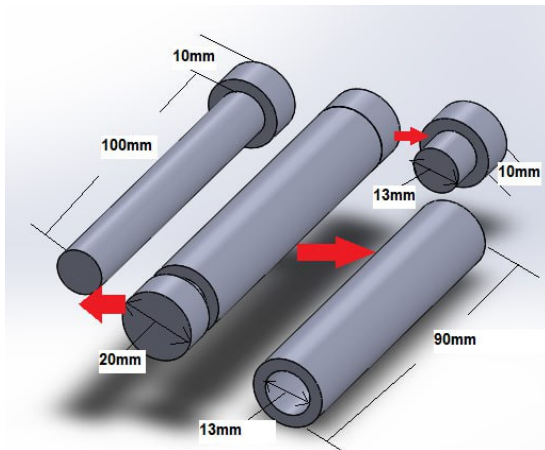
The percent weight ratio of the FGM layers is determined by one side with the higher percentage of aluminium while the other side has the higher rate of PTFE. Table 2 illustrates detailed information about the number of layers and powder contained in each FGM layer.

Table 2. Three different FGMs produced

Sample No.	Layer No.	Al wt%	PTFE wt%	Thickness of layer(mm)
FGM3	1	75	25	2
	2	50	50	5
	3	25	75	8
FGM2	1	75	25	1.5
	2	50	50	3.5
	3	25	75	4.5
	4	0	100	5.5
FGM1	1	100	0	1
	2	75	25	2
	3	50	50	3
	4	25	75	4
	5	0	100	5

2.2 Samples preparation

Developing the composite layers and the required functionally graded materials includes mixing the Al and PTFE powders, Compressing the mixture, staking layers, and sintering the green compact. According to the ratios in Table 2, the powder was weighted using a high-precision balance type (BEL) with a four-digit resolution. A ball blender was used to mix the constituents for one and a half hours to obtain a homogenous mixture using a Bench-Top planetary automatic ball mill (MTI Corporation). Four balls with 5 to 10 mm diameters were utilized to avoid the powder agglomeration.



(a)



(b)

Figure 3. (a) Powder compaction die parts lower punch, Upper punch, die chamber, and Die assembly (b) Hydraulic press.

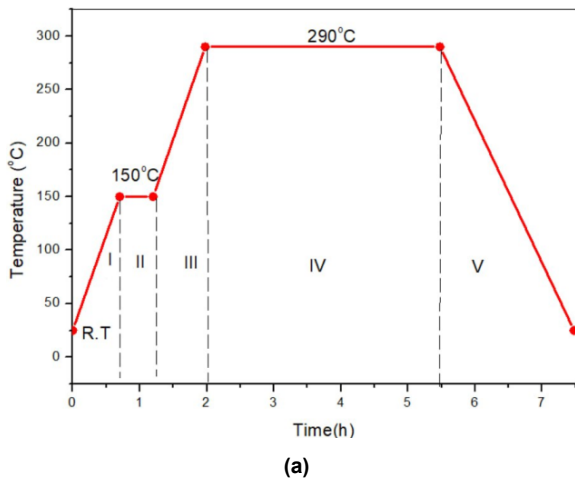
A cylindrical mold made of tool steel type BH224/5 with the chemical composition presented in Table 3 was used for stacking the powder mixture. The mold shown in Figure 3(a) consists of the cylindrical die chamber with inner and outer diameters of 13mm and 20mm, respectively, and a length of 150mm, upper punch with

Table 3. Chemical composition of tool steel

C%	Si%	Mn%	P%	S%	Cr%	Mo%	Ni%	Al%	Cu%	Fe%
0.466	0.268	0.637	0.0131	0.0269	0.950	0.208	1.53	0.0251	0.0567	Balance

a diameter of 13mm and a length of (100mm) and the movable lower punch with a diameter of 13mm. A careful layer-by-layer application was accomplished in the cylindrical Mold chamber with a 13mm diameter and 15 mm height, including three layers with (2mm, 5mm, and 8mm) sizes, respectively, four layers with sizes (1.5mm, 3.5mm, 4.5mm, 5.5mm), five layers with heights (1mm, 2mm, 3mm, 4mm, 5mm). The powder of each layer was poured into the die using a glass funnel, shaking the die to enhance its packing. The green samples are produced by uniaxially pressing the layers using a hydraulic press type Carver with a uniaxial pressing force of 6 tons applied on the mold piston using the hydraulic press shown in Figure 3(b). The green FGM samples are then sintered using an Argon inert atmosphere furnace according to the heating cycle shown in Figure 4(a) using the tumbler furnace with Argon inert atmosphere shown in Figure 4(b).

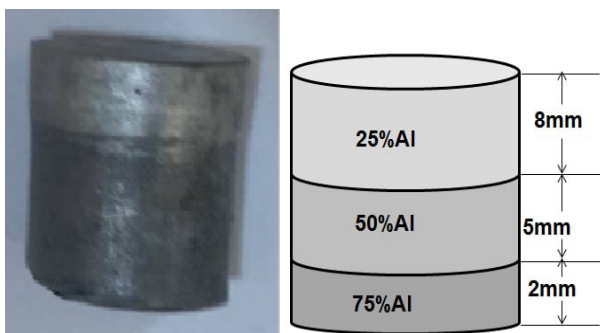
According to Figure 4(a), the program control of sintering temperature was divided into five stages. At stage I, the components of specimens were in solid phase, and the temperature of the specimen was increased to 150°C for 40 min with a heating rate of 3°C/min. In order to ensure the phase transformation of PTFE components in stage II, the end temperature is slightly lower than the melting point of PTFE. At stage II, the PTFE phase began to transform, and the transformation was accompanied by micro-cracks, which reduced the heating rate. The temperature increases to 290°C within 50 min in this stage, accelerating the melting flow. At stage III, the melting flow was kept for 30 min. At stage IV, the samples were left at 290°C for 210 minutes as while near the melting point of PTFE. Finally, in stage V, the temperature dropped from (290 to -120)°C for 120min. i.e., samples were left for 6 h in the furnace, the temperature was kept for half an hour and then cooled rapidly. The enhanced Al/PTFE reactive material specimen was obtained after the specimen was completely cooled. Enhanced Al/PTFE reactive material specimens have been obtained as a result of the sintering and rapid cooling of specimen structure. As a result of the mechanical pressing during the preparation of the specimens, it can noticed that before sintering, the distribution of each component in the specimen was not uniform, and the strength of the specimen in this stage was low. During the sintering process, PTFE was in the solid state, PTFE diffused between aluminum particles, the internal gap of the specimen became smaller, and some defects were eliminated. After this stage, the strength of the specimen was greatly improved. When the temperature was lower than the melting point of PTFE (290°C), the rapid cooling process was conducted after keeping for half an hour. At this stage, the volume of the specimen was reduced, the distribution was more orderly, and the internal defects of the specimen were further reduced; therefore, the strength of the specimen was further improved after this stage [31].



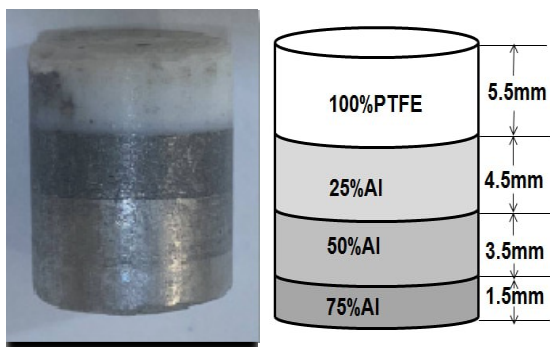
(b)

Figure 4. Sintering process (a) Sintering heat cycle (b) Tubler vacuuming furnace with an inert atmosphere.

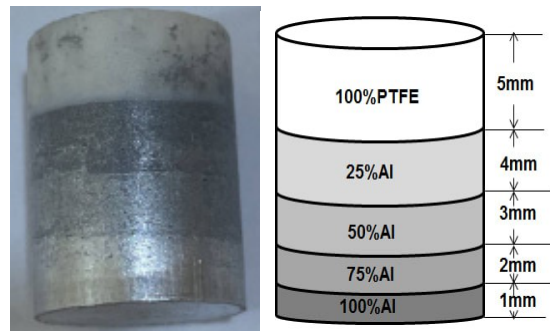
Figure 5 shows the three, four, and five layers of FGM samples produced after the sintering process.



(a)



(b)



(c)

Figure 5. Samples of FGM (a) Three layers, (b) Four layers, (c) Five layers

2.3 Apparent Density and porosity Measurement

The bulk density and porosity of the produced single layer and FGMs were measured experimentally using Archimedes principle (AP) according to ASTM C373-88 with the following steps:

1. The produced FGMs were dried inside a furnace at 110°C for 24 hours and cooled to room temperature. A sensitive balance is used to measure the dry mass (W_1).
2. The single layer and FGMs were hung in a distilled water bath, then boiled for five hours and soaked there for 24 hours. The suspended weight (W_2) was measured.
3. The water-saturated samples are then taken out of the water, and their surfaces are dried and weighed in air to obtain (W_3). The apparent density and porosity of the FGM can be calculated using the following formula [32]:

$$\rho_{ap} = \frac{W_1}{W_3 - W_2} \times \rho_w \quad (1)$$

where:

ρ_{ap} is the apparent density (g/cm^3)

ρ_w is the water density (g/cm^3)

The porosity of the FGM specimen can be calculated as [32]:

$$P\% = \frac{W_3 - W_1}{W_3 - W_2} \rho_w \quad (2)$$

where $P\%$ is the percentage of the apparent porosity.

The suspended and dry masses used in calculating the density and the porosity of the FGMs samples have been measured using the balance scale shown in Figure 6.



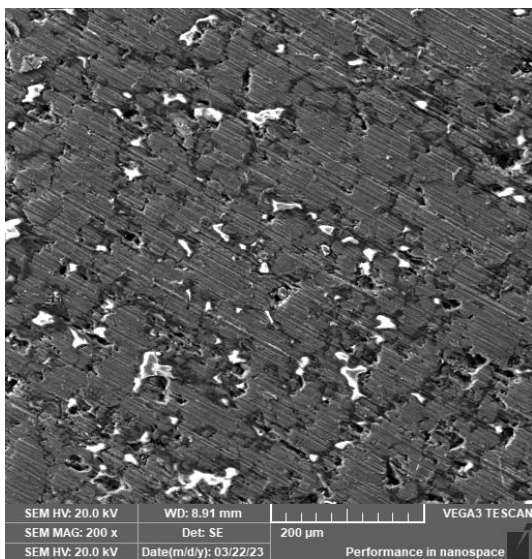
Figure 6. suspended mass and dry mass measurement

3. RESULTS AND DISCUSSION

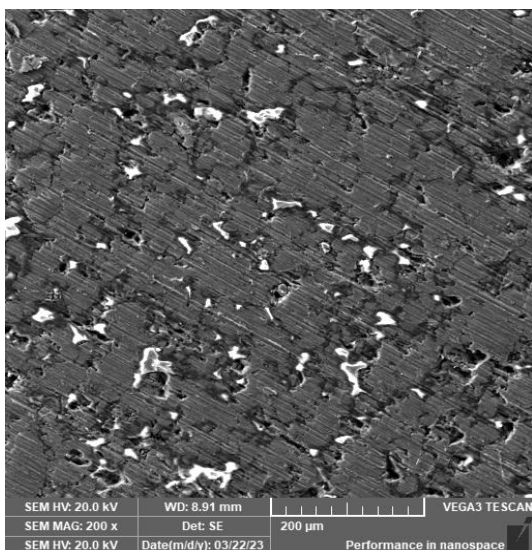
The following articles will discuss the results of XRD and microstructure for each layer and FGMs product and the measured density and porosity of such materials.

3.1 Microstructure results

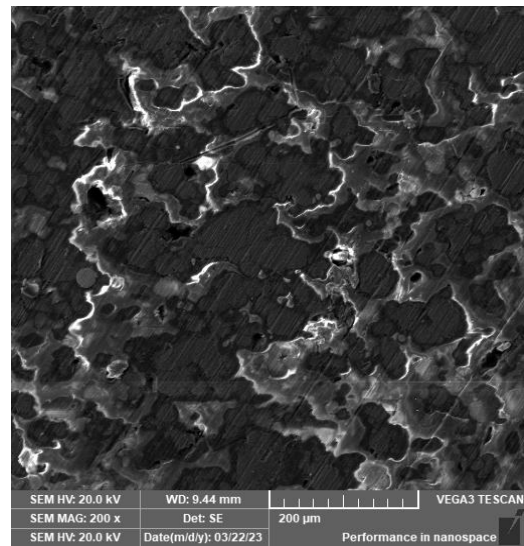
Figure 7 illustrates the SEM image for each layer of the FGM with 75wt%Al, 50wt%Al, and 25wt%Al, respectively, after performing the sintering process. Figure 7(a) shows the Aluminum matrix (black color) with a homogenous distribution of PTFE particles (white color) in a nearly rectangular shape at the grain boundaries of the Al. As illustrated in Figure 7 (b), more PTFE particles were displaced at the Al-matrix's grain boundaries by increasing the weight percentages of the PTFE particles. As can be observed from Figure 7(c), at a weight percentage of 75% for PTFE, there is a greater chance of PTFE particles aggregating at the outer boundaries of the aluminum grains. However, the PTFE particles are distributed uniformly throughout the aluminum matrix throughout these images, with no clustering.



(a)



(b)



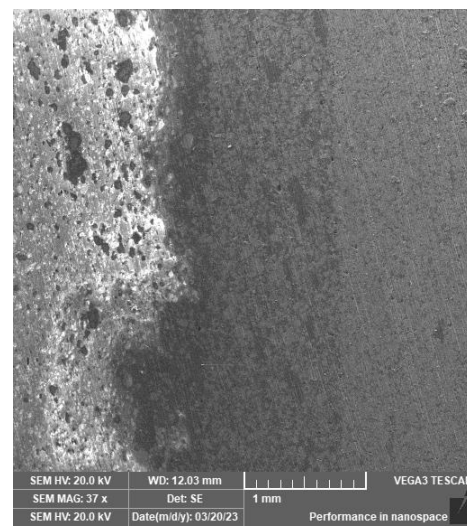
(c)

Figure 7. SEM image for single layer with chemical composition (a) 75%Al, (b) 50%Al, (c) 25%Al

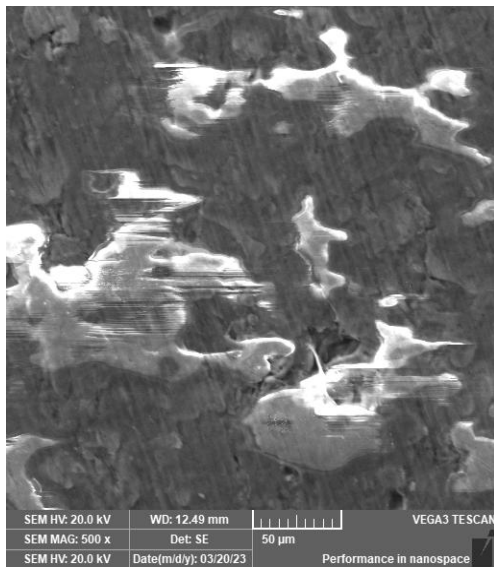
Figure 8 shows the SEM images for the functionally graded materials produced with three, four, and five layers. Figure 8(a) shows the strong diffusion between layers after sintering the three layers of FGM with clear inspected boundaries between them. Figure 8(b) and Figure 8 (c) show how the PTFE particles displaced within the Aluminium particles evenly. This can be attributed to the well preparation of the powder compaction.

3.2 XRD Characterization

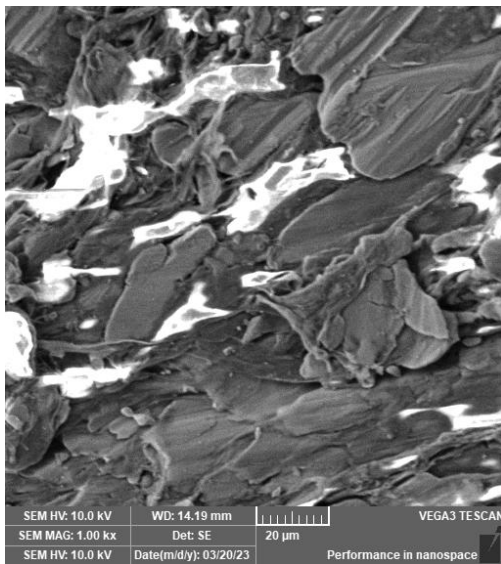
Three distinct produced FGMs layers, 75wt%Al-25wt%PTFE, 50wt%Al-50wt%PTFE, and 25wt% Al-75 wt% PTFE, were XRD tested after sintering as can be shown in Figures 9, Figure 10, and Figure 11. The XRD characterization was performed by comparing the acquired peaks with the diffraction after mixing the components. Since metal-polymer FGM layers were developed in the current work, it is unlikely that the elements will interact. However, the peak shift between the Al and PTFE, as well as their composites, which have various weight percentages of both elements, reveals that the synthesized product experienced a structural change.



(a)



(b)



(c)

Figure 8. SEM images of produced FGM (a) Three layers, (b) Four layers, (c) Five layers

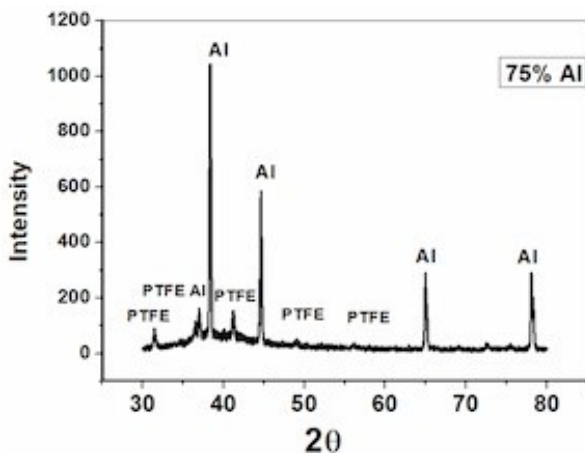


Figure 9. XRD for the layer with 75%Al and 25% PTFE

The XRD analysis presented in Figure 9 shows that all acquired peaks have been shifted to the left when comparing them with those of the aluminum illustrated in Figure 1(b). This Figure reveals that the layer consists

of 75%Al and 25% PTFE particles after sintering has an angle $2\theta = 31.3^\circ, 37^\circ, 38^\circ, 41.1^\circ, 49^\circ, 37.1^\circ, 65^\circ$ and 78° while it becomes $22.5^\circ, 31.1^\circ, 37.1^\circ, 38^\circ$ and 66° for a layer consists 50% Al and 50% PTFE as can be shown in Figure10 and $2\theta=31.8^\circ, 37.1^\circ, 38.5^\circ, 41.5^\circ, 44.5^\circ, 65.5^\circ, 78^\circ$ for the layer consists of 25%Al and 75% PTFE as illustrated in Figure11. The comparison of the peak positions of the different layers with those of Al ($2\theta=38.1^\circ, 45^\circ, 65.5^\circ, 78^\circ$) shows that the peaks of the composite materials shifted to the left, which reveals an expansion of the material crystallin. The SEM image for the five layers of FGM shown in Figure 12 clearly depicts the displacement of the PTFE particles inside the Aluminium matrix.

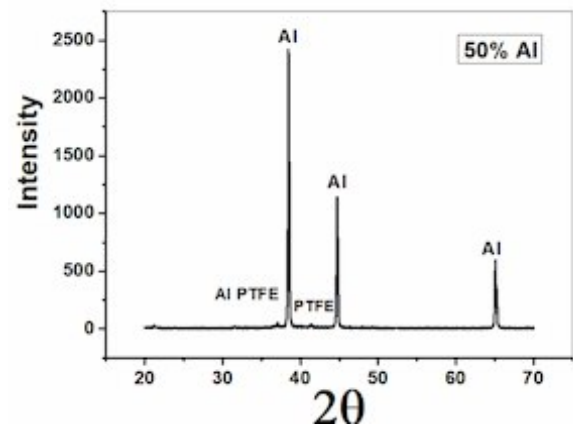


Figure 10. XRD for the layer with 50%Al and 50% PTFE

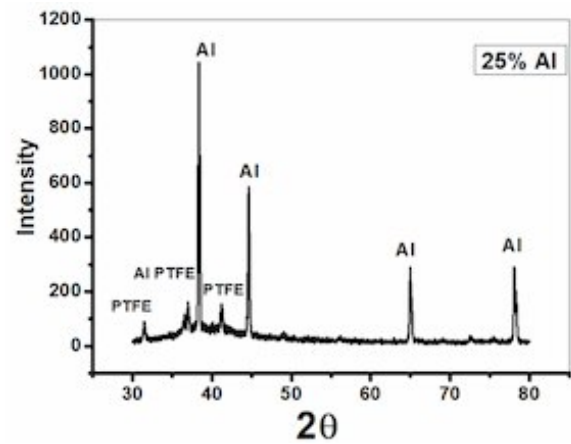


Figure 11. XRD for the layer with 25%Al and 75% PTFE

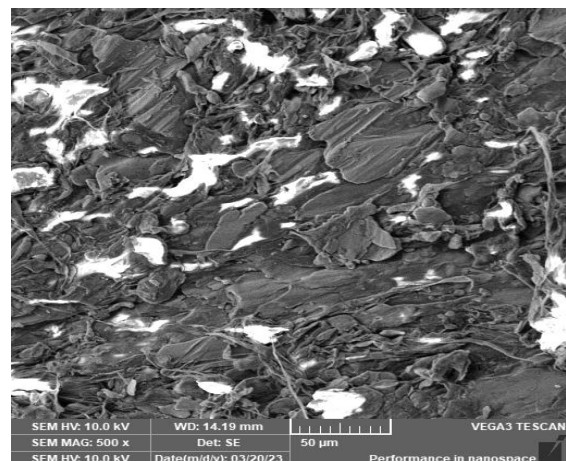


Figure 12. SEM images of produced Five layers of FGM

3.3 Results of Density Measurement

Each layer's bulk density and the material that has been functionally graded have been measured using the method outlined in section 2.3. The results obtained for three, four, and five layers of FGM are demonstrated in Figures 14 to 17.

3.4 Hardness measurement

Hardness values across the wall thickness of the samples were made between the PTFE-rich and Aluminium-rich regions. Figure 13 illustrates the average values of the microhardness of PTFE-Al layers with different Al particle content. This Figure shows that the hardness increases with the increased percentage of the Aluminium particles. The hardness improved from 6.37HV in a PTFE-rich layer (with zero Al particle content) to 51.35HV in an Aluminium-rich layer (25wt% of PTFE and 75wt% of Al). The hardness improvement can be attributed to the good mechanical properties of the Al compared to the PTFE. As shown in Figures 7-12, the nearly homogeneous distribution of the PTFE helps improve this.

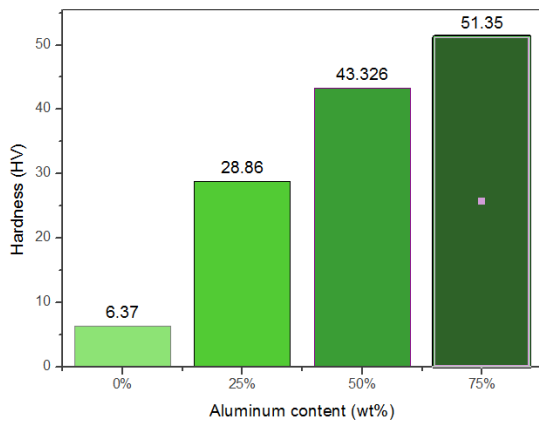


Figure 13. Average microhardness of the different composite layers

Figure 14 shows that the apparent density of the three layers of FGM is 2.254 gm/cm³ as compared to 2.068 gm/cm³ and 2.246 gm/cm³ for four and five layers of FGMs, as can be seen from Figure 15 and Figure 16. It was observed that when compared to the three layers of FGM, the apparent density of the four FGMs decreased by 8% while the density of the five layers of FGM negligibly increased by 0.35%.

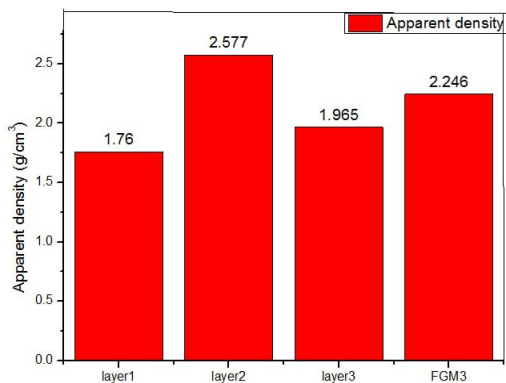


Figure 14. Apparent density for three layers of FGM

The drop in density for the four layers of functionally graded materials can be attributed to the FGM's increased porosity, as can be observed in the SEM images of the various layers that were previously provided. Figure 17 compares the apparent densities of various functionally graded materials to those of their primary components (Al and PTFE). This graph demonstrates that the apparent densities of the various functionally graded materials produced are more comparable to those of PTFE than Al.

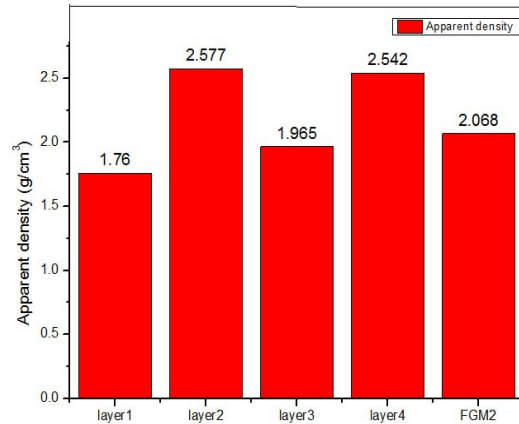


Figure 15. Apparent density for four layers of FGM

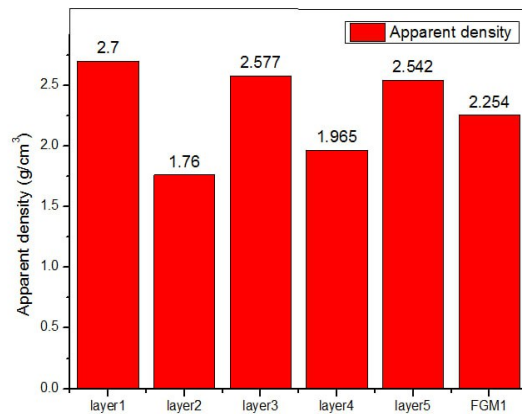


Figure 16. Apparent density for Five layers FGMs

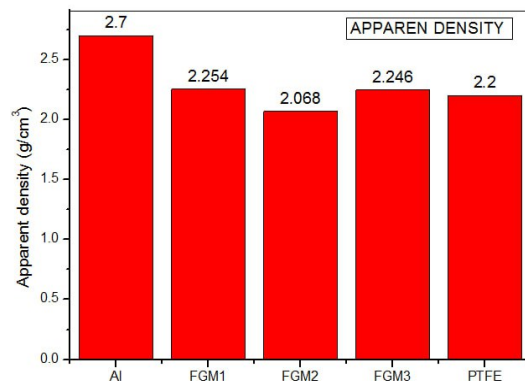


Figure 17. Comparison between the apparent density of different FGMs

3.5 Results of the porosity measurement

Figures 18 to 20 show the results of the measurements performed on the porosity of the various layers as well as the functionally graded materials using the method described in section 2.4. Figure 18 demonstrates that the

highest porosity for layer one, composed of 75wt% Aluminium and 25wt% PTFE, is 1.76%, whereas the porosity for the other two layers is minimal and only reaches 0.6525%. Also, this Figure shows that the FGM with three layers has a porosity of 2.31% greater than the three layers. Figure 19 illustrates each layer's porosity and the four FGM layers. This Figure displays a porosity of 0.297% for the first layer, which made up 75wt%Al and 25wt%PTFE, while it becomes 0.6525wt% for the second and third layers, which are composed of 50wt%Al-50wt%PTFE and 25wt%Al-75wt%PTFE respectively. The fourth layer shows a porosity of 4.49%, which represents the highest porosity even than the four layers FGM, which exhibited a 2.27% porosity. Figure 20 demonstrates that the first and fifth layers of the FGM exhibited the highest porosities, with respective values of 2.7% and 4.94%, compared to the other three layers. The functionally graded material shows an overall porosity of 1.818%, which is lower than the porosity of the top and bottom layers. As can be seen, the functionally graded material with five layers has a lower porosity of 1.818% compared to that of three and four-layer FGMs, which reached 2.13% and 2.27%. A comparison between the porosities of various functionally graded materials is shown in Figure 21. This Figure clearly shows that the porosities of different FGMs are nearly comparable to that of Al rather than the PTFE. Comparatively speaking, the five-layer FGM (FGM₁) exhibits the most negligible porosity. The porosity of FGM₁ reaches 1.818%, with 3.8% higher than Al's, while FGM2 and FGM3 show 29.71% and 21.71% higher than Al.

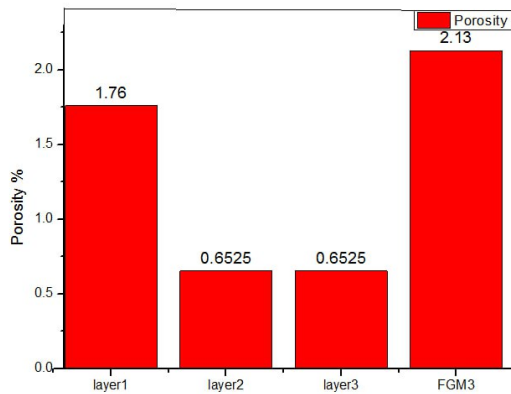


Fig. 17. Three layers of FGM porosity

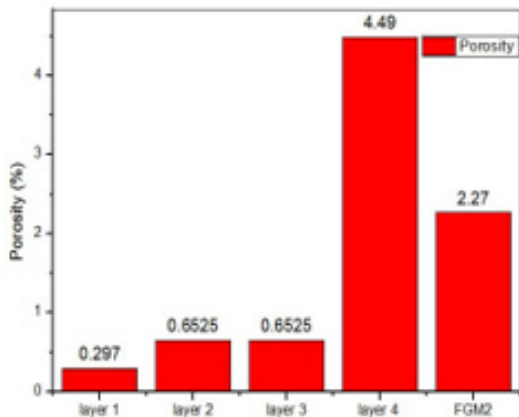


Figure 19. Four layers of FGM porosity

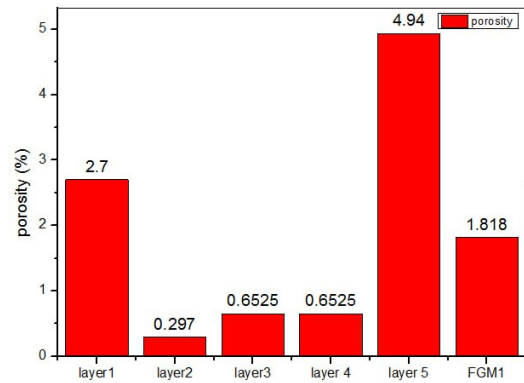


Figure20. Five layers of FGM Porosity

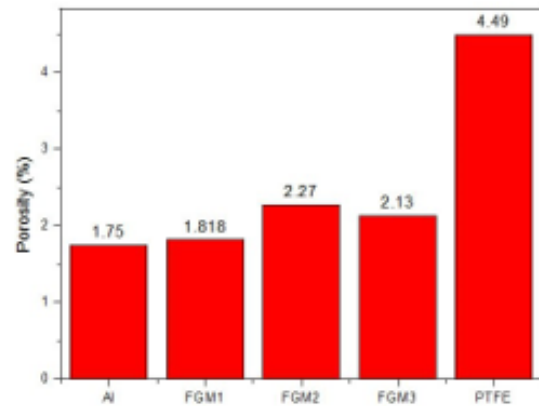


Figure 21. Porosity of different FGMs

4. CONCLUSIONS

The present work has produced three different Al-PTFE functionally graded materials with three, four, and five layers using uniaxial powder compaction technology. The materials are characterized by checking the microstructure and measuring the porosity and the apparent densities for the different layers and the FGMs. Following is a summary of the findings related to the microstructure, density, and porosity of the produced functionally graded materials:

1. Functionally graded materials with three, four, and five layers have been successfully produced using the powder compaction technique without delamination in transition boundaries and surface defects.
2. The hardness improved from 6.37HV in a PTFE-rich layer to 51.35HV in an aluminum-rich layer.
3. SEM images confirm the strong diffusion of the layer boundaries.
4. The PTFE particles distributed relatively homogeneously in Al particles when added with low concentrations (25% and 50%), while they agglomerated at the Al boundaries when added with a higher concentration (75%).
5. The SEM images of the different functionally graded materials produced confirm the change in host particle size. XRD results indicated the possibility of distortion in the crystal lattice.
6. The apparent density of different functionally graded materials is comparable to that of the PTFE rather than Al.
7. The highest and the lowest apparent densities were observed at the layers containing 50 wt% and 25 wt%PTFE, respectively.

8. The highest and the lowest porosities were observed with the four and five-layer FGMs, respectively.

REFERENCES

- [1] M.I.A. Latiff, D.M. Nuruzzaman, S. Basri, N.M. Ismail, S.N.S. Jamaludin, F.F. Kamaruzaman: Preparation and characterization of 6-layered functionally graded nickel-alumina (Ni-Al₂O₃) composites, IOP Conf. Series: Materials Science and Engineering, Vol.342, 012063,2018.[http:// doi.org: 10.1088/1757-899X/342/1/012063](http://doi.org/10.1088/1757-899X/342/1/012063)
- [2] Y. Li et al: A Review on Functionally Graded Materials and Structures via Additive Manufacturing: From Multi-Scale Design to Versatile Functional Properties, Adv. Mater. Technol, Vol.5, 1900981, 2020. <https://doi.org/10.1002/admt.201900981>
- [3] R.S. Parihar, R. Kumar Sahu, S.G. Setti: Finite Element Modelling of Functionally Graded Cemented Tungsten Carbide Compaction with Flow Stress Estimation, Materials Today: Proceedings, Vol. 5, pp.7009-7018,2018.<https://doi.org/10.1016/j.matpr.2017.11.364>
- [4] I. Kayabasi, G. Sur, H. Gokkaya, Y. Sun: Functionally Graded Material Production and Characterization using the Vertical Separator Molding Technique and the Powder Metallurgy Method, Engineering, Technology and Applied Science Research, Vol.12, No.4, pp.8785-8790,2022.<https://doi.org/10.48084/etasr.5025>
- [5] R.S. Parihar, S.G. Setti, R. Kumar Sahu: Recent advances in the manufacturing processes of functionally graded materials: A review, Sci Eng Compos Mater, Vol.25, No.2, pp.309-336,2018. [http:// DOI.org /10.1515/secm-2015-0395](http://DOI.org/10.1515/secm-2015-0395)
- [6] I.M. El-Galy, B.I. Saleh, M. Ham-ed: Functionally graded materials classification and development trends from an industrial point of view, SN Applied Sciences, Vol.1, No. 1378, 2019, <https://doi.org/10.1007/s42452-019-1413-4>
- [7] R. Gupta, et al: Mechanical and microstructural characterization of W-Cu FGM fabricated by one-step sintering method through PM route, IOP Conf. Series: Materials Science and Engineering, Vol. 338, 012042, 2018.[http://doi.org: 10.1088/1757-899X/338/1/012042](http://doi.org/10.1088/1757-899X/338/1/012042)
- [8] S. Farahmand, A.H. Monazzah, M.H. Soorgee: The fabrication of Al₂O₃-Al FGM by SPS under different sintering temperatures: Microstructural evaluation and bending behaviour, Ceramics International 2019. <https://doi.org/10.1016/j.ceramint.2019.07.318>
- [9] M.I.A. Latiff, S.N.S. Jamaludin, S. Basri, A. Hussain, D.S. Alothmany, F. Mustapha, D.M. Nuruzzaman, N.M. Ismail, I. Ismail: Effect of Sintering Temperature on Functionally Graded Nickel /Alumina Plate, Applied Mechanics and Materials, Vol.629, pp.437-443,2014.[https:// doi.org/10.4028/www.scientific.net/AMM.629.437](https://doi.org/10.4028/www.scientific.net/AMM.629.437)
- [10] V .Boggarapu, L. Ruthik, D. Kumar Gara, S. Ojha, S. Jain, R. Gujjala, A. Kumar Bandaru, R. Inala: Study on mechanical and tribological characteristics of layered functionally graded polymer composite materials, Proceedings of the Institution of Mechanical Engineers, Part E: Journal of Process Mechanical Engineering, Vol. 236, No.5. 2022, <http://doi.org/10.1177/09544089221074841>
- [11] V. Boggarapu, R. Gujjala, S. Ojha, S. Acharya, P. V. Babu, S. Chowdary, D. kumar Gara: State of the art in functionally graded materials, Composite Structures, Vol.262, pp.113596, 2021.<https://doi.org/10.1016/j.compstruct.2021.113596>.
- [12] The Metal-polymer Bearing Solution Challenges and Lessons Learned, Report sponsored by GGB, <https://www.azom.com/article.aspx?ArticleID,21216>
- [13] Y. Yang, et al: Friction-induced construction of PTFE-anchored MXene heterogeneous lubricating coating and its in-situ tribological transfer mechanism, Chemical Engineering Journal, Vol.442, pp. 13623, 2022, <https://doi.org/10.1016/j.cej.2022.136238>
- [14] J.-X. Wu et al: Investigation on Mechanical Properties and Reaction Characteristics of Al-PTFE Composites with Different Al Particle Size, Advances in Materials Science and Engineering, pp.1-10,2018. <https://doi.org/10.1155/2018/2767-563>
- [15] M. Sahli, A. Cablé, K. Chetehouna, S. Hamamda, N. Gascoin, S. Revo: Preparation and Characterization of Polytetrafluoroethylene (PTFE)/ Thermally Expanded Graphite (TEG) Nanocomposites, Article in Composites Part B Engineering 2017. <https://doi.org/10.1016/j.compositesb.2017.05.046>
- [16] M. Sam: Development of functionally graded Cu-Sn-Ni/Al₂O₃ composite for bearing applications and investigation of its mechanical and wear behavior, Particulate Science and Technology 2017. [http://dx .doi.org/ 10.1080 /02 726351.2017. 136431 2.](http://dx.doi.org/10.1080/02726351.2017.1364312)
- [17] N. Radhika, R. Reghunath, M. Sam: Improvement of mechanical and tribological properties of centrifugally cast functionally graded copper for bearing applications, Proc IMechE Part C: J Mechanical Engineering Science, Vol.0, No.0, pp.1-12, 2018 ,<https://doi.org/10.1177/0954406218805508>
- [18] P.N.S. Srinivas et al: Microstructural, mechanical and tribological characterization on the Al-based functionally graded material fabricated powder metallurgy, Mater. Res. Express, Vol.7, pp. 026513, 2020. <https://doi.org/10.1088/2053-1591/ab6f41>
- [19] A. Khoddamzadeh: Development of Lead-free PTFE Based Sliding Bearing Materials, A thesis submitted to The Faculty of Graduate Studies and Research in partial fulfilment of the degree requirements of Master of Applied Science Ottawa-Carleton Institute for Mechanical and Aerospace Engineering 2007.
- [20] Xiao Wang, Junwei Wu, Luhai Zhou, Xicheng Wei and Wurong Wang: Tribological behaviours of amino-functionalized graphene reinforced PTFE composite, Proc IMechE Part J: J Engineering Tribology; Vol.0, No.0, pp.1-9,2018. [https:// doi.org/ 10.1177 / 1350650117754000](https://doi.org/10.1177/1350650117754000)

- [21] T. Tevruz: Tribological behaviours of bronze-filled polytetrafluoroethylene dry journal bearings, *Wear*, Vol.230, pp. 61–69,1999. [https://doi.org/10.1016/S0043-1648\(99\)00091-5](https://doi.org/10.1016/S0043-1648(99)00091-5)
- [22] R. Wang, J. Huang, Q. Liu, S. Wu, J. Wu, X. Ren, Y. Li: The effect of particle size and mass ratio on the mechanical response of Al/PTFE/SiC composite with a 2³ factorial design, *RSC Adv.* 2022; 12: 2810–2819, <https://doi.org/10.1039/D1R A07985A>
- [23] A.B. Bhosale, M.V. Walame, M. Lathesh: Influence of Different Parameters on the Specific Wear Rate of PTFE Composites in the Steam Environment, *IOP Conf. Series: Materials Science and Engineering* 2022; 1272:012019, <http://doi.org/10.1088/1757-899X/1272/1/012019>
- [24] H. Hu, Y. He, Q. Wang, L. Tao: Investigation of in-situ tribological performance of Polyimide-MoS₂/PTFE composite under atomic oxygen irradiation, *tribology-international* 2023,108437. <https://doi.org/10.1016/j.triboint.2023.108437>
- [25] I. Zidaru, R.G. Ripeanu, I. Tudor, A.C. Drumeanu: Research Regarding the Improvements of Tribological Behavior in Three Cone Bits Bearings, *FME Transactions*, Vol. 37, No. 2, pp. 99-102, 2009.
- [26] R. Keshavamurthy, V. Tambrallimath, A. Badari, A.R. Krishna, P.G.S. Kumar, M.C. Jeevan: Friction and Wear Behaviour of Copper Reinforced Acrylonitrile Butadiene Styrene based Polymer Composite Developed by Fused Deposition Modelling Process, *FME Transactions*, Vol. 48, pp. 543-550, 2020.
- [27] S. Kumar Soni, B. Thomas: Microstructure, Mechanical Properties and Machinability Studies of Al7075/SiC/h-BN Hybrid Nanocomposite Fabricated via Ultrasonic-assisted Squeeze Casting, *FME Transactions*, Vol.48, pp.532-542, 2020.
- [28] C. Fragassa, G. Minak, M. Sassatelli: Reducing Defects in Composite Monocoque Frames, *FME Transactions*, Vol.47, pp.48-53, 2019.
- [29] D.J.C. Dhas, S. Senthilnathan, G. Manivannan, N. Azhagesan: Extensive Investigation in Wear Behavior of Alumina-PTFE Composite for Medical Implant Applications, *International Journal of Composite Materials*, Vol. 7, No.4, pp. 115-119, 2017.
- [30] R. M. Nasir, B.T. Ting, A. Y. Saad: Dry/wet Sliding Activation Wear of Pure Al, *Journal of Mechanical Engineering*, Vol. SI 1 (1), 157-174, 2017.
- [31] E. Tang, Z. Sun, Y. Han, W. Yu, C. Chen, M. Xu, M. Chang, K. Guo, L. He: Dynamic characteristics of enhanced Al/PTFE and real-time quantitative evaluation of impact release energy under vacuum environment, *Results in Physics* 31, 105019, 2021.
- [32] ASTM C373- 88, Standard Test Method for Water Absorption, Bulk Density, Apparent Porosity, and Apparent Specific Gravity of Fired Whiteware Products, 2006.

NOMENCLATURE

P	Apparent porosity(percentage)
W_1	the dry mass (gm)
W_2	The suspended weight (gm)
W_3	Mass of the sample in the air (gm)
ρ_{ap}	Apparent density (g/cm ³)
ρ_w	Water density(g/cm ³)

Abbreviations

Al	Aluminum
SiC	Silicon carbide
FGM	Functionally graded material
MoS ₂	Molybdenum die sulphate
PTFE	Poly-tetra-fluoro-ethylene
SEM	Scanning electron microscope
XRD	X-ray diffraction

СИНТЕТИКА И КАРАКТЕРИЗАЦИЈА АЛ-ПТФЕ ФУНКЦИОНАЛНО КЛАСИФИКОВАНОГ МАТЕРИЈАЛА ПРИМЕНОМ ТЕХНИКЕ МЕТАЛУРГИЈЕ ПРАХА

Г.Х. Омран, Н.С. Ратхи, Б.А. Абас

Тренутни рад укључује производњу функционално класификованог материјала (Ал-ПТФЕ) применом технике металургије праха. Предложени грађирани материјали укључују три, четири и пет слојева. Сваки слој се састоји од ПТФЕ и Ал честица просечног пречника од 200 нм и 25 микрометара, респективно. Прахови су помешани, формирану у цилиндричне облике, а затим синтеровани у пећи у инертној средини. Микроструктурне и морфолошке особине класификованих материјала су проучаване коришћењем КСРД и СЕМ слика. Експериментално се мери густина и тврдоћа припремљених класификованих материјала. Резултати КСРД и СЕМ снимака откривају да су ФГМ-ови успешно развијени без икаквог раздвајања или стварања пукотина и да је ПТФЕ био равномерно диспергован по слојевима са концентрацијама честица од 25 и 50 теж.%. Ал. Добијени резултати такође откривају да је густина различитих ФГМ упоредива са густином ПТФЕ.